Aqua MODIS: 20 Years of On-orbit Calibration and Performance

Xiaoxiong Xiong,[a*], Amit Angal,[b] Tiejun Chang,[b] Emily Aldoretta, [b]
Xu Geng,[b] Daniel Link,[b] Junqiang Sun,[b] Kevin Twedt,[b] and Aisheng Wu[b]
[a] Sciences and Exploration Directorate, NASA GSFC, Greenbelt, MD 20771
[b] Science Systems and Applications Inc., 10210 Greenbelt Road, Lanham, MD 20706

Abstract. Since its launch in May 2002, Aqua MODIS has successfully operated for more than 20 years and has continuously generated a wide range of data products that have enabled and supported the remote sensing community and users worldwide for their studies of the Earth's system by monitoring changes in its key environmental parameters. Although Aqua MODIS, designed with a lifetime requirement of 6 years, is currently operated in its extended mission phase, it continues to make high quality global observations of the Earth's surface via its 36 spectral bands that cover wavelengths from visible to long-wave infrared. To date, all instrument on-board calibrators (OBC) remain capable of performing their design functions, providing various calibration data sets to help monitor on-orbit changes in sensor responses and performance characteristics. In addition to the OBC, regularly scheduled lunar observations and select Earth-view targets are used extensively to support sensor on-orbit calibration, especially for the calibration of the visible channels (or bands). In this paper, we provide an overview of Aqua MODIS on-orbit calibration activities and methodologies for both reflective solar bands (RSB) and thermal emissive bands (TEB), illustrate its on-orbit performance over the past 20 years using examples derived from OBC measurements, lunar observations, and Earth-view response trends, and describe various calibration improvements made over its entire mission. We focus on key issues identified since launch, such as solar diffuser degradation, electronic crosstalk, and on-orbit changes in sensor response versus scan-angle, along with approaches and strategies developed to mitigate their impact on sensor calibration quality. Also discussed in this paper are some of the key calibration enhancements incorporated recently in the Collection 6.1 and the upcoming Collection 7 Level-1B algorithms.

Keywords: Aqua, MODIS, calibration, on-board calibrators, lunar observations, response versus scan-angle, polarization

***First Author**, E-mail: xiaoxiong.xiong-1@nasa.gov

*Contact Author, E-mail: amit.angal@ssaihq.com

1 Introduction

Aqua Moderate Resolution Imaging Spectroradiometer (MODIS) has successfully operated for more than 20 years since its launch on May 4, 2002. Nearly 40 science products are routinely generated from the MODIS observations, including those made by Terra MODIS (launched in 1999). MODIS is a key instrument for the NASA's Earth Observing System (EOS) Terra and Aqua missions. It was designed and developed based on the remote sensing community's requirement to extend and enhance the data records established by heritage sensors such as the Advanced Very High Resolution Radiometer (AVHRR), the Nimbus 7 Coastal Zone Color Scanner (CZCS), the

Sea-Viewing Wide Field-of-View Sensor (SeaWiFS), the NOAA High Resolution Infrared Radiation Sounder (HIRS), and the Landsat Thematic Mapper (TM). In comparison with its heritage sensors, MODIS had more stringent calibration requirements and a suite of on-board calibrators designed to help meet these requirements on-orbit [1-2].

MODIS is a scanning radiometer collecting data in 36 spectral bands via a two-sided scan mirror. Its observations are made at 3 spatial resolutions (nadir): 250 m for bands 1-2, 500 m for bands 3-7, and 1 km for bands 8-36. Table 1 is a summary of the key design specifications of the MODIS spectral bands. The reflective solar bands (RSB; bands 1-19 and 26) are calibrated by a solar diffuser (SD) and solar diffuser stability monitor (SDSM) system, coupled with regularly scheduled lunar observations and long-term response trends over pseudo-invariant calibration sites (PICS). The thermal emissive bands (TEB; bands 20-25 and 27-36) are calibrated by referencing an on-board blackbody (BB). The on-orbit changes in sensor spectral and spatial characteristics are monitored by a spectro-radiometric calibration assembly (SRCA) [3-4].

Table 1 Key design parameters for the MODIS spectral bands

Primary Use	Band[1]	Bandwidth (nm)	Spectral Radiance[2]	Required SNR	Primary Use	Band[1]	Bandwidth (µm)	Spectral Radiance[2]	Required NEΔT(K)
Land/Cloud/Aerosols Boundaries	1	620 - 670	21.8	128	Surface/Cloud Temperature	20	3.660 - 3.840	0.45 (300K)	0.05
	2	841 - 876	24.7	201		21	3.929 - 3.989	2.38 (335K)	0.2
Land/Cloud/Aerosols Properties	3	459 - 479	35.3	243		22	3.929 - 3.989	0.67 (300K)	0.07
	4	545 - 565	29	228		23	4.020 - 4.080	0.79 (300K)	0.07
	5	1230 - 1250	5.4	74	Atmospheric Temperature	24	4.433 - 4.498	0.17 (250K)	0.25
	6	1628 - 1652	7.3	275		25	4.482 - 4.549	0.59 (275K)	0.25
	7	2105 - 2155	1	110	Cirrus Clouds Water Vapor	26	1.360 - 1.390	6	150 (SNR)
Ocean Color/ Phytoplankton/ Biogeochemistry	8	405 - 420	44.9	880		27	6.535 - 6.895	1.16 (240K)	0.25
	9	438 - 448	41.9	838		28	7.175 - 7.475	2.18 (250K)	0.25
	10	483 - 493	32.1	802	Cloud Properties	29	8.400 - 8.700	9.58 (300K)	0.05
	11	526 - 536	27.9	754	Ozone	30	9.580 - 9.880	3.69 (250K)	0.25
	12	546 - 556	21	750	Surface/Cloud Temperature	31	10.780 - 11.280	9.55 (300K)	0.05
	13	662 - 672	9.5	910		32	11.770 - 12.270	8.94 (300K)	0.05
	14	673 - 683	8.7	1087	Cloud Top Altitude	33	13.185 - 13.485	4.52 (260K)	0.25
	15	743 - 753	10.2	586		34	13.485 - 13.785	3.76 (250K)	0.25
	16	862 - 877	6.2	516		35	13.785 - 14.085	3.11 (240K)	0.25
Atmospheric Water Vapor	17	890 - 920	10	167		36	14.085 - 14.385	2.08 (220K)	0.35
	18	931 - 941	3.6	57	[1] Spatial resolution: 250m (B1-2), 500m (B3-7), 1000m (B8-36)				
	19	915 - 965	15	250	[2] Spectral Radiance unit: W/m^2-µm-sr				

Aqua MODIS underwent intensive prelaunch characterization with measurements made in a thermal vacuum environment to characterize the detector gain, dynamic range, response non-linearity, signal-to-noise ratio (SNR), noise equivalent temperature difference (NEdT), and other key parameters. Numerous lessons learned from the Terra MODIS design and development phases have contributed to the superior on-orbit performance of Aqua MODIS. In particular, the large out-of-band thermal leak and electronic crosstalk observed in Terra MODIS prelaunch characterization were largely mitigated in Aqua MODIS due to extensive efforts from the instrument vendor [5-6].

In this paper, we provide an overview of Aqua MODIS on-orbit operation and calibration activities spanning the last two decades. We illustrate the calibration performance along with discussions on the major calibration improvements in the upcoming reprocess of the MODIS Level-1B (L1B) data record, Collection 7 (C7) [7]. After more than 20 years of on-orbit operations, the on-board calibrators (OBC), including the SD, SDSM, BB, and SRCA, continue to be routinely operated and provide the baseline calibration and characterization for Aqua MODIS [8-9]. Finally, the lessons learned from Aqua MODIS, remaining challenges, and future improvements are discussed. The Aqua MODIS on-orbit operation has significantly exceeded its design lifetime of 6 years and, despite the on-orbit changes in the sensor responses, it continues to meet the needs of the science community to generate high quality data products.

2 Instrument Operation and Calibration Activities

Since launch, the Aqua spacecraft and its MODIS instrument have been in continuous operations, with a few exceptions. Shortly after launch, the spacecraft encountered two brief safe-hold periods in June 2002, due to single event upsets. In recent years, the system has begun to show its age and has experienced a few anomalies. An unexpected transition to upload mode caused the MODIS formatter to reset in January 2018, causing some unexpected changes in detector performance. The spacecraft has also begun to show issues associated with its prolonged exposure to the space environment, which have manifested in the way science data is stored on the spacecraft. A flexible-multiplexer unit (FMU) anomaly occurred in August 2020, preventing science data from MODIS and other instruments from being saved correctly before data downlink. The Aqua flight operations team performed a reset of the FMU to regain its functionality in September 2020, with MODIS commanded into standby mode during the recovery. A similar issue with the FMU and solid-state recorder (SSR) occurred in February 2022, requiring a similar reset in March 2022. At the end of the same month (March 31, 2022), the Aqua spacecraft transitioned to a safe-hold state, causing MODIS to transition into safe hold. The spacecraft recovery occurred a few weeks later, with MODIS returning to science mode on April 13, 2022. This was followed by an outgas cycle to remove any potential contamination that may have built up during the safe hold period. The full list of key Aqua MODIS instrument events is listed in Table 2.

Table 2 Major Events for Aqua MODIS

Date	Event	Description
May 4, 2002	Launch	Vandenberg Air Force Base, California
June 7, 2002	Science Mode	MODIS transitions to science mode
June 24, 2002	First Light	Nadir door open
June 27, 2002	S/C Safe Hold	Spacecraft single event upset (returned to science mode on July 2)
July 29, 2002	S/C Safe Hold	Spacecraft ground pointing anomaly (returned to science mode on August 6)
January 4, 2018	Formatter Reset	The MODIS formatter reset after an unexpected transition to upload mode.
August 6, 2020	FMU Anomaly	An anomaly with the spacecraft flexible-multiplexer unit (FMU) led to instrument science data losses (reset with MODIS in standby on September 2)
February 22, 2022	FMU/SSR Anomaly	An anomaly with the spacecraft FMU and solid-state recorder (SSR) caused intermittent losses in science data (reset with MODIS in standby on March 23)
March 31, 2022	S/C Safe Hold	Spacecraft single event upset (returned to science mode on April 13 post an outgas)

Aqua MODIS performs calibrations on a regular basis to properly track the performance of its detectors and to aid the MODIS Characterization Support Team (MCST) in generating updates to calibration coefficient look-up tables (LUTs). The SDSM is nominally operated on a 3-week basis, with each calibration having a pair of SD screen open and SD screen closed measurements. BB warm-up cool-down (WUCD) cycles are performed once per quarter [10]. Observations of the Moon are scheduled on a near monthly basis and are available with the aid of a spacecraft roll maneuver, with a lunar phase angle between 55 and 56 degrees chosen to obtain repeatable observation conditions. Due to these and other limiting factors, on an average, 9-10 lunar observations are available per year [11]. Out-of-turn calibrations are also possible and are performed on an as-needed basis in response to instrument anomalies, spacecraft anomalies, and unexpected changes in detector performance. The SRCA provides a source for various calibrations in its radiometric, spatial, and spectral modes. Radiometric mode calibrations are currently performed quarterly while spatial and spectral calibrations are currently performed twice per year [12-13]. These calibration frequencies have been adjusted throughout the mission based on the limited lifetimes of some of these calibrators and the observed rate of change of detector gain.

Overall, the Aqua MODIS instrument has performed quite well. Table 3 shows the number of each calibration performed throughout the mission. As noted earlier, there have only been a few instrument issues experienced on-orbit, with the majority due to spacecraft anomalies. The temperatures of the instrument and ambient (non-temperature controlled) focal plane arrays (FPAs) have shown steady performance with only a slight (<2K) drift since launch with a similar seasonal oscillation (<2K), which can be seen in Figure 1. The only significant issue Aqua has experienced on orbit has been its loss of cold focal plane (CFPA) cooler margin, which was first observed in 2011. The lack of cooler margin prevented the CFPAs from being held at their set point continuously. Over the next few years, further loss of cooler margin led to increased average CFPA temperatures, which can also be seen in Figure 1. However, the thermal bands on these FPAs derive their gain coefficient on a per-scan basis and much of the effect of the temperature change was mitigated [14]. Aqua MODIS began to regain cooler margin in mid-2013 and by 2015 showed significant improvement. The outgas operation as part of the MODIS recovery after the most recent 2022 safe hold led to a complete recovery in the CFPA temperature performance.

Table 3 Aqua MODIS on-orbit calibration activities (as of March 31, 2023)

Type of calibrations	Number of operations
SD/SDSM	801
BB WUCD	90
SRCA (radiometric)	204
SRCA (spatial)	82
SRCA (spectral)	56
Lunar	213

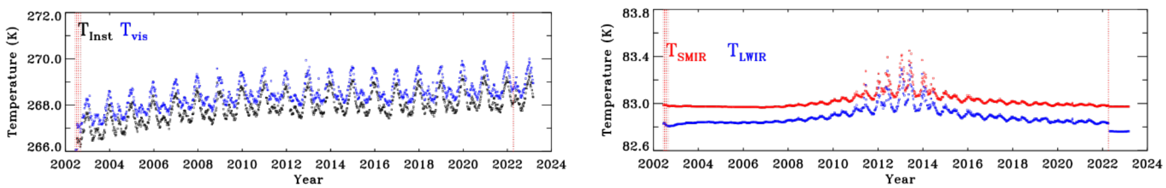

Fig. 1 (left) Aqua MODIS instrument (black) and VIS FPA (blue) temperature trends. (right) Aqua MODIS short and midwave infrared (SMIR; red) and longwave infrared (LWIR; blue) FPA temperature trends. Red vertical dotted lines represent safe hold occurrences.

In January 2022, the Aqua spacecraft exited the A-train constellation. Originally planned to be a series of spacecraft retrograde burns, the Aqua spacecraft has ceased station-keeping burns and will drift for the next several years until science operations conclude. As part of this extended science period, MODIS calibrations will continue. As the missions have continued to operate beyond their designed life of 6 years, the calibration methodology, particularly at short wavelengths has involved the use of Earth view responses from repeatable observations of the pseudo invariant calibration sites (PICS). MCST expects additional calibration efforts will be required to monitor the performance of the instrument as the geometries of any Earth-viewing calibrations will shift due to the loss of the 16-day repeatable Earth observations that were present for most of the mission.

3 On-Orbit Performance

3.1 RSB Radiometric Performances

The SD reflectance has decreased over the mission due to the periodic exposure to solar radiation during the scheduled SD/SDSM calibration events, as well as some indirect exposure to solar stray light through the nadir port. The degradation of the SD has been reliably tracked by the SDSM system for the last two decades [15-16]. Figure 2(a) shows the time evolution of the SD degradation, which is the SD reflectance relative to its value at launch, at different wavelengths as measured by three of the nine SDSM detectors. There is more degradation for shorter wavelengths, with the shortest wavelength detector 1 (410 nm) showing 22% drop in reflectance as of March 2023. Figure 2(b) shows the SD degradation as a function of wavelength at three different points in time over the mission. The wavelength dependence is roughly described by a power law function with a power of about -4. The power law dependence is used to extend the measured SDSM degradation from the near infrared (NIR) detectors to the short-wave infrared (SWIR) wavelengths to estimate the SD degradation for the MODIS SWIR bands, though this remains very small for Aqua MODIS [17].

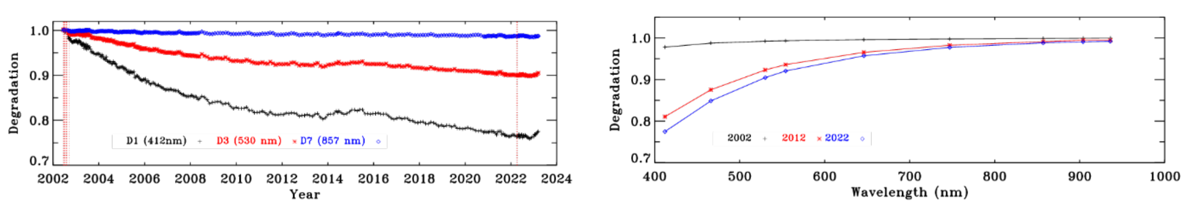

Fig. 2 Degradation in the reflectance of the solar diffuser over the mission as measured by the SDSM. (Left) The measured SD degradation at SDSM detectors 1, 3, and 7 as a function of time.

(Right) The SD degradation as a function of wavelength for three select years during the mission. Red vertical dotted lines represent safe hold occurrences.

The SD measurements, after correcting for the SD degradation, remain the primary source for calibrating the RSB detector gains. Observations of the Moon are also made on a regular basis as an independent way of tracking changes in RSB detector gain over the mission. Since the SD and lunar measurements are made at different angles of incidence (AOI) of the scan mirror, the difference between the SD-derived and lunar-derived gain changes provides a measure of the mirror's response versus scan angle (RVS) change on orbit [7]. Figure 3 shows examples of SD and lunar on-orbit gain changes for visible (VIS) bands 8 (412 nm), 3 (469 nm), and 4 (555 nm) over the mission. The shortest wavelength bands have the largest changes in both gain and RVS, with band 8 showing a 38% gain change in the SD measurements as of March 2023. Figure 4 shows the on-orbit gain changes from the SD measurements for several NIR and SWIR bands. In general, the longer-wavelength bands have smaller gain changes compared to the shorter-wavelength VIS bands. The April 2022 safe hold event resulted in a sharp gain change in the SWIR band responses, particularly for bands 5 and 26. SD measurements taken days after recovery from safe hold showed a sudden gain increase of a few percent for these bands, followed by a gradual decrease over the next year and stabilization near the pre-safe-mode levels.

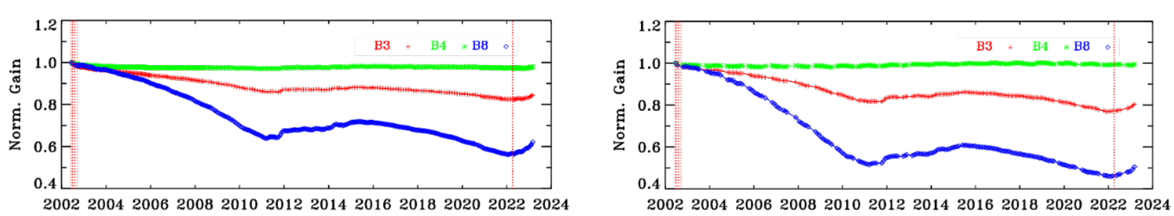

Fig. 3 On-orbit gain changes for VIS bands 8, 3, and 4 from (left) SD measurements and (right) lunar observations. Red vertical dotted lines represent safe hold occurrences.

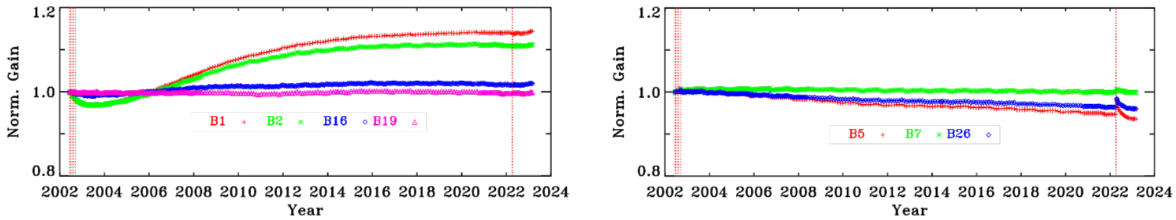

Fig. 4 On-orbit gain changes from SD measurements for (left) NIR bands 1, 2, 16, and 19 and (right) SWIR bands 5, 7, and 26. Red vertical dotted lines represent safe hold occurrences.

On-orbit changes in the scan mirror RVS are estimated for the complete set of view angles using linear extrapolation from SD and lunar measurements. For some bands, particularly at shorter wavelengths, Earth-scene reflectance trends have shown large on-orbit changes that are not accounted for with a linearly determined RVS. Furthermore, the non-uniformity in the SD degradation with respect to the incident and outgoing directions also results in an inadequacy in the gain determination from the SD measurements. For bands 1-4 and 8-9, supplemental data from PICS in the Libya desert are used to track MODIS gain changes at several different view angles across the entire MODIS scan range. The desert data is used to derive a correction to the m_1 (inverse of the instrument gain) and RVS calibration relative to the on-board calibrators. The data are fit to a quartic function versus frame to determine the final RVS [18-19]. Examples of the evolution of the RVS function over the mission are shown in Figure 5 for bands 8 (412 nm), 3 (469 nm), and 1 (645 nm). The RVS on-orbit change is largest for band 8 and has been more stable for longer wavelength bands. Compared to Terra MODIS, the on-orbit gain, mirror side differences, and RVS changes have been less significant for the Aqua RSB. The Aqua RSB have also not shown any indication of a change in polarization sensitivity, which has been a significant problem for the short-wavelength Terra RSB since the middle of the Terra mission [20-21].

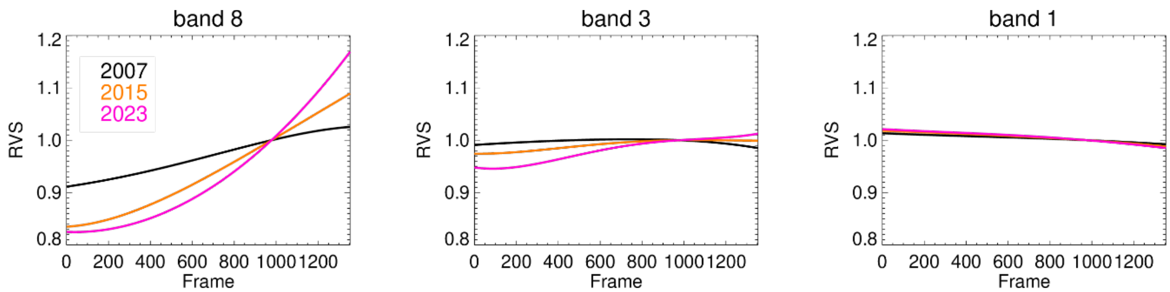

Fig. 5 RVS for (left) band 8, (center) band 3, and (right) band 1 at three different times in the mission. By definition, the RVS is normalized to the SD frame (978).

Except for band 6, there have been no new inoperable RSB detectors since the beginning of the mission. For band 6, several of the detectors were inoperable since pre-launch testing and the status of some detectors has changed periodically over the mission. Most recently, after the 2022 safe hold event, an additional band 6 detector was flagged as inoperable, leaving only 7 of the 20 detectors classified as operable. The noise performance of most RSB detectors has remained excellent throughout the mission. The SNR at typical radiance has remained above the specified requirements for all RSB except band 8, where the large drop in gain on-orbit has led to a corresponding drop in SNR [22]. Table 4 presents the yearly-averaged SNR performance for the RSB. The SNR is determined from SD measurements taken throughout each year. Yearly SNR is shown relative to the specification, so values above unity have an SNR above specification.

Table 4 RSB SNR Performance at typical radiance. Yearly-averaged results are shown relative to their band specification.

Band	Spec	2002	2012	2022	Band	Spec	2002	2012	2022
1	128	1.54	1.67	1.79	12	750	2.04	1.98	1.97
2	201	2.53	2.77	2.79	13L	910	1.58	1.64	1.68
3	243	1.32	1.19	1.14	13H	910	1.82	1.90	1.94
4	228	1.42	1.42	1.42	14L	1087	1.45	1.47	1.49
5	74	2.05	1.97	1.94	14H	1087	1.80	1.84	1.85
6	275	1.64	1.57	1.79	15	586	2.67	2.72	2.78
7	110	1.40	1.41	1.42	16	516	2.78	2.87	2.90
8	880	1.27	0.89	0.77	17	167	2.20	2.23	2.25
9	838	1.84	1.54	1.41	18	57	1.60	1.63	1.63
10	802	1.94	1.79	1.74	19	250	2.04	2.05	2.06
11	754	2.29	2.24	2.24	26	150	1.86	1.86	1.88

MODIS employs a reflectance-based calibration with the accuracy requirements of ±2% in reflectance and ±5% in radiance for the RSB for scan angles within ±45° at typical radiance. An additional 1% uncertainty is allowed for scan angles outside this range and radiance (L) levels from $0.3L_{typ}$ to $0.9L_{max}$. To assess the compliance to these requirements, the uncertainty impact from each parameter of the MODIS RSB calibration algorithm was measured prelaunch and is routinely assessed on-orbit. Recently, a comprehensive review of the MODIS RSB uncertainty was published and included prelaunch and on-orbit measurements together with a summary of the uncertainty performance. Figure 6 shows the uncertainty for all RSB for select years at typical radiance and nadir AOI. Except for a few short-wavelength bands that rely on desert targets for RVS characterization, the on-orbit uncertainty for the MODIS RSBs is seen to be within the 2% reflectance specification [23].

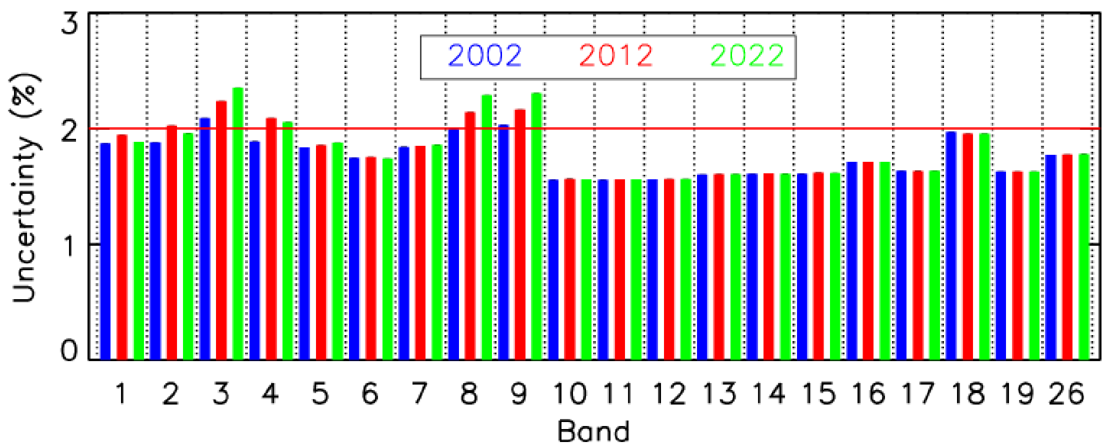

Fig. 6 Aqua MODIS RSB uncertainty at nadir (typical radiance) for select years. The horizontal red line indicates the specified 2% uncertainty requirement.

3.2 TEB Radiometric Performances

The TEB calibration algorithm uses a quadratic function to convert digital output to radiance. The offset value, a_0, used in the current Collection 6.1 (C6.1) L1B product, was determined prelaunch. The quadratic coefficient (a_2) is updated by adding adjustments to the prelaunch results using the on-orbit BB WUCD. The linear coefficient (b_1) is calculated on-orbit on a scan-by-scan basis in reference to a temperature-controlled BB at 285 K along with a deep-space view. Trends of the BB temperature shown in Figure 7 demonstrate the excellent short-term and long-term stability of the BB as a calibration source [24].

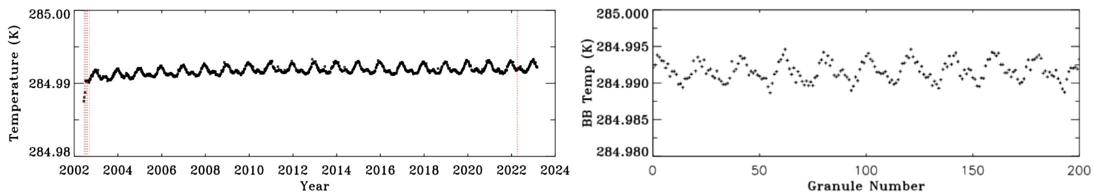

Fig. 7 (Left) Trend of Aqua BB temperature over the mission. Data are collected at weekly intervals. (Right) BB temperature collected using 200 consecutive granules on July 3, 2022. Red vertical dotted lines represent safe hold occurrences.

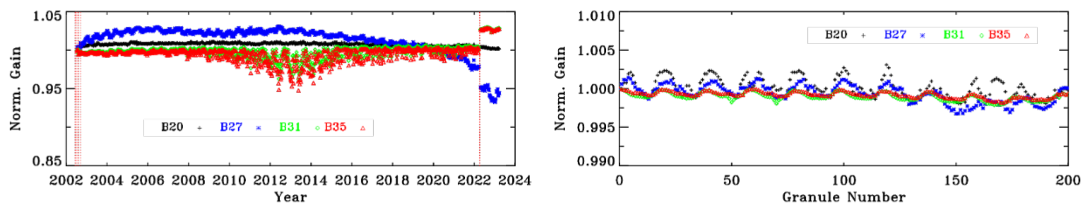

Fig. 8 (Left) Trends of normalized 1/ b_1 (gain) over the mission for Aqua bands 20, 27, 31 and 35. Data are collected at weekly intervals. (Right) Normalized b_1 for the same four bands collected using 200 consecutive granules on July 3, 2022. Red vertical dotted lines represent safe hold occurrences.

Figure 8 shows the normalized gain (1/ b_1) trends for Aqua bands 20, 27, 31 and 35. For bands 31 and 35, variations in gain have been observed since 2006 due to the gradual loss of the CFPA temperature cooler margin discussed in Section 2. Fluctuations in gain over a short time period on a granule-by-granule basis show variations of up to ±0.2%, depending on the band. Small uncertainties in BB, mirror side, instrument, and cavity temperature measurements are expected to have additional impacts on the gain calculation. Figure 8(a) also highlights large, discontinuous changes in gain for several TEB (band 27, 31 and 35, shown) at the time of the 2022 safe hold event. Electronic crosstalk among the detectors in the photovoltaic (PV) LWIR bands (27-30) has been observed for both Terra and Aqua MODIS with lower signal contamination observed in Aqua MODIS when compared against Terra MODIS [25]. An increase of the crosstalk influence on gain can be seen with band 27 in Fig. 8(a) starting in 2015 and becoming more significant over time. A correction to the crosstalk in these bands was developed using data from lunar observations and is included in C6.1 and C7 (discussed in Section 4). The recovery from the 2022 safe hold required a reset of the MODIS electronics and resulted in a change in the characteristics of the PV LWIR crosstalk. Crosstalk corrections are currently applied to both calibration and Earth measurements in the L1B product to account for these changes. On top of the lunar-derived crosstalk coefficients, an additional crosstalk adjustment is derived using Earth measurement assessments and applied to the coefficients to further reduce striping in the L1B imagery. Separately, the gain change in bands 31 and 35 following the safe hold event is likely due to instrument nonlinear response changes after outgassing.

The NEdT values measured at the typical radiance, used to assess TEB detector noise characteristics, are shown in Table 5, where all band values (average of operable detectors) are lower than their specified NEdT. Results indicate stable short-term and long-term performance of the TEB. For Aqua band 27, the sudden jump in NEdT in 2022 is due to an immediate increase in the crosstalk contamination following the safe hold event. Currently, except for a few detectors that are classified as noisy, the NEdT values of the TEB are well within the requirements set at the typical radiance. Band 21 is primarily used for fire detection but has the highest NEdT relative to its specification [26].

Table 5. Aqua MODIS TEB noise performance (at typical temperature) for select years

Band	20	21	22	23	24	25	27	28	29	30	31	32	33	34	35	36
Spec	0.05	0.2	0.07	0.07	0.25	0.25	0.25	0.25	0.05	0.25	0.05	0.05	0.25	0.25	0.25	0.25
2002	0.02	0.2	0.02	0.02	0.11	0.04	0.1	0.05	0.02	0.09	0.02	0.03	0.08	0.12	0.15	0.23
2012	0.02	0.19	0.02	0.02	0.11	0.04	0.1	0.05	0.02	0.09	0.02	0.03	0.08	0.12	0.15	0.23
2022	0.02	0.19	0.02	0.02	0.1	0.04	0.12	0.05	0.02	0.11	0.02	0.02	0.08	0.12	0.15	0.22

The TEB calibration uncertainty, which is shown for select years in Figure 9, is determined by combining the contributions from various parameters involved in the BB calibration and calculation of the Earth view (EV) radiance. The uncertainty associated with each parameter is assumed to be independent and the total uncertainty is estimated as the root mean square summation of all contributions. While some of the parameters were determined from prelaunch calibration and characterization, others are derived and updated from on-orbit measurements. Special considerations are given to crosstalk effects with an additional penalty being applied at the pixel level. As can be seen from Figure 9, all TEB continue to meet the specification [23].

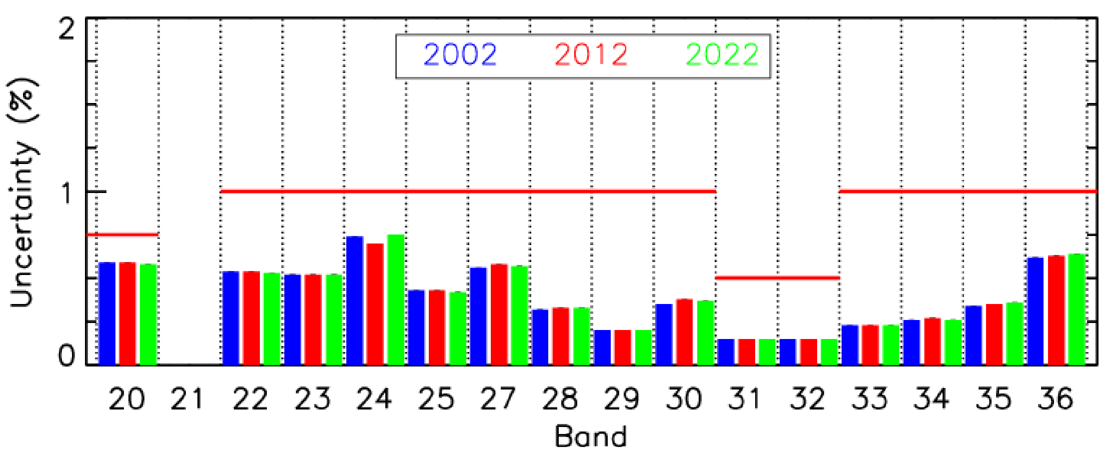

Fig. 9 Aqua MODIS TEB uncertainty at nadir (typical radiance) for the years 2002, 2012, and 2022. The horizontal red lines indicate the specified uncertainty requirement for each band.

3.3 *Spatial and Spectral Performance*

Using the results of regular calibrations performed by the SRCA, we have monitored the spatial and spectral performance of the Aqua MODIS bands throughout the mission. The results presented in Figures 10 and 11 are band and yearly averaged results from the SRCA calibrations from select years. Data from the current year (2023) is not shown due to the tendency of seasonal oscillations to skew partial-year results. This is particularly true in the spatial results, which show a seasonal variation matching the changes in the instrument and VIS/NIR FPA temperatures. The SRCA spatial calibration can monitor the performance of all 36 MODIS bands while the spectral calibration is limited to bands with wavelengths less than 1 μm. The spatial performance is assessed by band-to-band registration (BBR), noting the center of each sensing band/detector relative to band 1. The most significant feature of the Aqua MODIS BBR is the shift between CFPAs relative to the NIR FPA (where band 1 is located). The shift of over 200 m in the instantaneous field of view was measured during pre-launch testing in both the along-scan and along-track directions. Another shift was observed when comparing the prelaunch measurements to the early measurements on-orbit, believed to be due to the stresses of reaching orbit. Minor shifts in the BBR have been observed during on-orbit operations and have not shown impact to downstream data products. The yearly-averaged BBR values for select years are shown in Figure 10 [27].

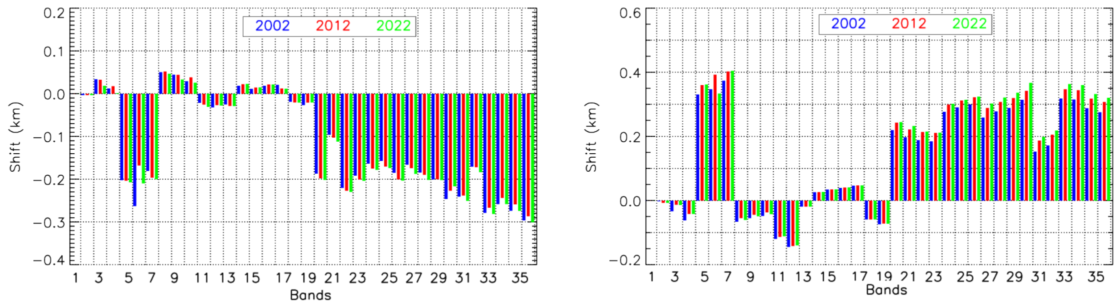

Fig. 10 The yearly-averaged BBR along-scan (left) and along-track (right) for all Aqua MODIS bands for select years.

The RSR for Aqua MODIS bands was characterized as part of the pre-launch testing program. The SRCA, in its spectral calibration mode, can produce light at tuned wavelengths from 0.4 to 1µm, which allows for on-orbit RSR characterization for 15 of the MODIS bands. Results from spectral calibrations are compared with pre-launch measurements to determine changes in the RSR CW and BW for those bands. The values presented are the average of multiple spectral calibrations that took place during each calendar year. Three representative years spanning the mission were chosen and the spectral performance was characterized by noting changes in the measured band center wavelength (CW) and bandwidth (BW) as shown in Figure 11. The CW for most measured bands has remained stable, with only slight drifts of < 0.5 nm over the course of the mission. However, some bands, particularly those with a larger BW (bands 1, 17, and 19 have 30 to 50 nm BW compared to the 10 to 20 nm bandwidth of most other RSB) have shown shifts in BW of up to 1 nm. Additionally, the loss of three of the four available 10 W SRCA lamps has reduced the effective output of the SRCA, particularly during spectral calibrations. As such, the performance of some of the VIS bands (e.g., band 3 and 8) are less accurately characterized by the SRCA in recent years (results are omitted for band 8 CW and BW after 2006, and band 3 BW after 2016) [28].

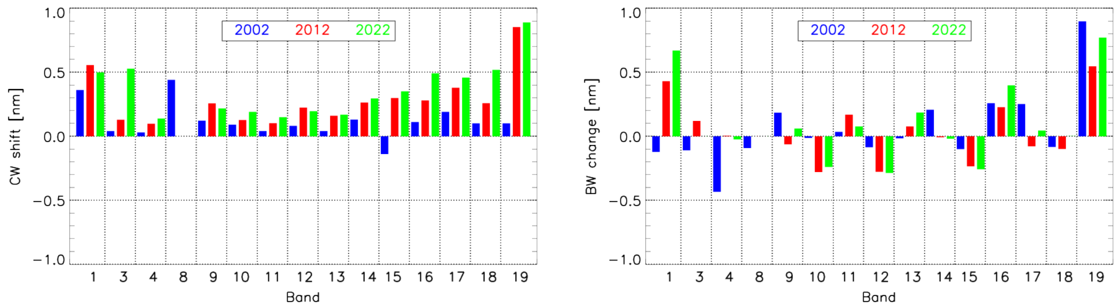

Fig. 11 The yearly-averaged CW (left) and BW (right) changes in the Aqua MODIS RSB for select years.

4 Recent Calibration Improvements

The MODIS L1B software, developed and maintained by the MCST, is used to convert the raw sensor data into calibrated reflectance and radiance for the downstream science products. Continuous efforts are dedicated to algorithm enhancements and look-up-table updates to ensure the quality of the L1B product. A new collection is periodically initiated when significant improvements are made to the L1B, achieved through either improved instrument characterization, a breakthrough of the calibration methodology, special handling to account for an instrument anomaly, inputs from MODIS science disciplines, or a software upgrade. Each new data collection requires mission reprocessing of the MODIS L1B as well as many key science products to establish the long-term data product consistency. More details of the L1B algorithms and their evolution in previous collections are well documented in previous publications [29]. The latest operational L1B version, C6.1, was triggered by the development of an effective crosstalk correction algorithm for Terra MODIS PV LWIR bands [30]. For Aqua, the most significant algorithm improvement in C6.1 was the extension of the use of desert data in the RSB RVS calibration to include bands 1-4. This approach had previously been applied in Collection 6 to bands 8 and 9 only. The Aqua Collection 6.1 forward processing started in September 2017.

The Collection 7 L1B code and LUT were made available for science testing by MCST in early 2021. For C7, several major changes were made to the L1B code as well as the calibration algorithms used to generate the RSB and TEB coefficient LUTs. The major L1B code change was the implementation of the electronic crosstalk correction to PV LWIR and MWIR bands. The crosstalk correction was applied to all detectors of Aqua MODIS bands 27 – 30. The crosstalk effects in the Aqua MWIR bands (except band 21) were only dominant in detector 1 and as a result a correction based on lunar observations was applied [7]. A revised uncertainty algorithm was developed and implemented to account for the uncertainty due to the crosstalk correction. L1B code changes were also made to enable crosstalk corrections at the very beginning and end of the scan range, and to improve the dynamic range for some short-wavelength RSB, restoring pixels that were erroneously flagged as out of dynamic range in the previous versions [7]. Furthermore, all MODIS data products in C7 will be produced in NetCDF4/HDF5 and HDFEOS-5 instead of HDF4 and HDFEOS-2 that have been used from the start of the mission. The application programming interface (API) has been developed by the NASA's Land Data Operational Products Evaluation (LDOPE) team to facilitate the data format transition in all levels of MODIS data processing.

In addition to these L1B code changes, several changes were made to the calibration algorithms used to generate the RSB and TEB LUTs for Collection 7. For the RSB, the Collection 7 algorithm and LUTs are very similar to what was used in Collection 6.1 for Aqua MODIS, though Terra MODIS has more significant changes [31]. The desert PICS continue to be used to derive an EV-based calibration for bands 1-4 and 8-9, as in Collection 6.1, but changes were made to the processing and fitting of the desert data for Collection 7. The desert observations from different view angles of a site are binned per month, fit first over frame (or AOI), and then fit over time. The data from three sites – Libya 1, Libya 2, and Libya 4 – are processed and fit separately and then combined to derive the final RVS. These processing and fitting changes were made partly to prepare for changes to the frequency and repeatability of desert site observations as the Aqua orbit drifts away from its historic ground track and inclination plane. Additionally, an improved characterization of the Aqua MODIS SD screen vignetting function is used in Collection 7, which reduces the seasonal oscillations in the SD measured gain values, making it easier to track short-term changes for the ocean bands 8-16, the bands that use SD screen closed calibrations. The RSB LUTs are reprocessed over the mission for C7 using a consistent calibration algorithm and fitting strategy, which provides a smoother calibration, removing the uncertainties of forward prediction inherent in the current C6.1 LUTs. The combined effect of the fitting improvements and reprocessing leads to a more stable reflectance product in C7. This is illustrated in Figure 12, which shows the near-nadir reflectance trends and reflectance mirror side ratio trends of band 8 over the Libya 4 site for C6.1 compared to C7. The C7 trends are more stable over the mission.

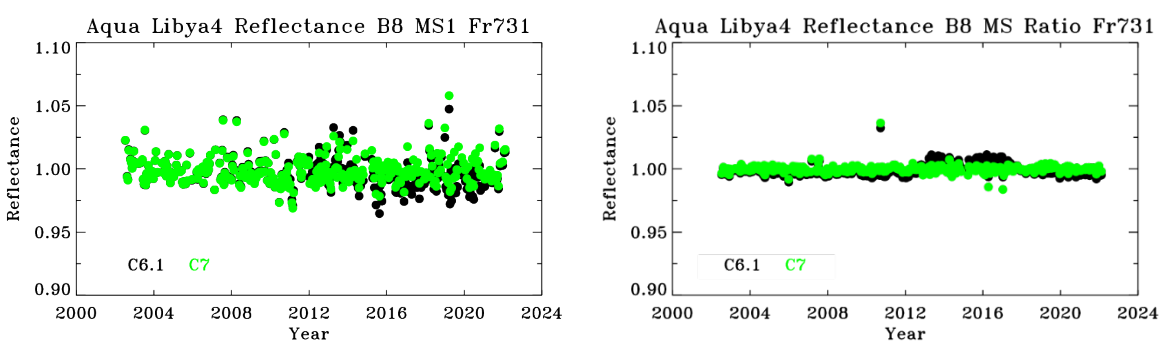

Fig. 12 : (Left) Libya 4 reflectance trends for Aqua band 8 mirror side 1 frame 731 (near nadir) for Collection 6.1 compared to Collection 7. (Right) Comparison of C6.1 to C7 reflectance mirror side ratio.

For the TEB, the Collection 7 algorithm includes several major improvements [32]. Evidence of electronic crosstalk contamination has been observed in lunar images from both the MWIR and LWIR bands as well as Earth-scene imagery, and the contamination has increased over the mission for many bands. The magnitudes of the contamination showed a significant increase for the Aqua PV LWIR bands, 27-30, after the instrument underwent a safe-mode event in March 2022. A correction for the electronic crosstalk effect is applied for selected detectors in the MWIR bands and all the detectors in the PV LWIR bands 27, 29, and 30 throughout the entire mission in C7. For band 28, the crosstalk correction is only applied after the 2022 safe hold event. The correction for all PV LWIR bands has also been applied in the C6.1 L1B in the forward production after the March 2022 safe hold event. Figure 13 (left) illustrates the L1B image quality improvement for Aqua band 24 detector 1 in comparison with other detectors before and after the crosstalk correction. Figure 13 (right) shows a similar histogram comparison for Aqua band 27 using a post safe-mode granule. A significant improvement for several detectors in band 27 can been seen after the crosstalk correction.

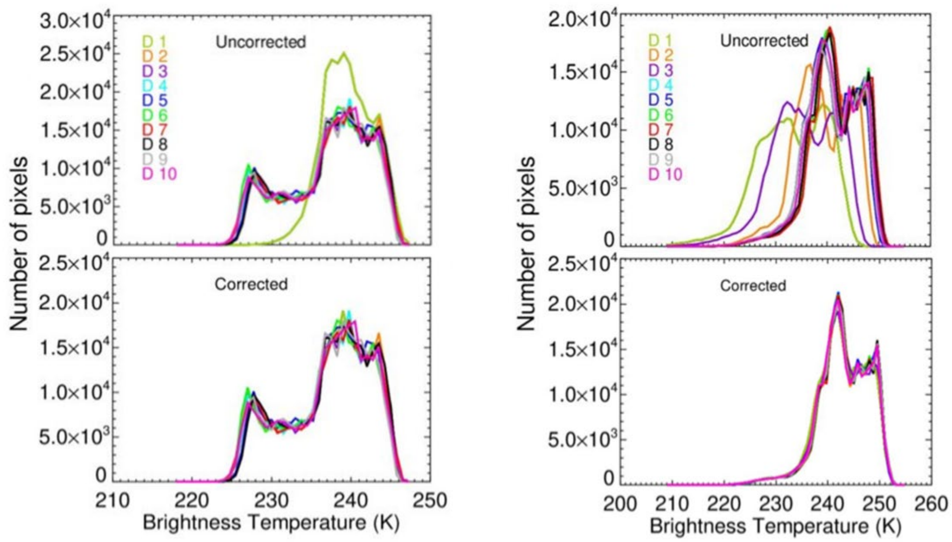

Fig. 13: (Left) Comparison of histograms for Aqua band 24 detector 1 before and after the electronic crosstalk correction using granule 2023034.0020. (Right) Comparison of histograms for all detectors of Aqua band 27 using granule 2023062.1200.

Analysis of C6.1 brightness temperature (BT) differences between the two mirror sides using nighttime quasi-deep convective clouds (qDCC) indicate the differences at extreme low temperature could be up to 2.0 K depending on the band, particularly for the MWIR and PV LWIR bands. A formatter reset event that occurred on January 2018 was found to cause a significant change in the mirror side BT difference. To correct for the mirror side differences, a time-dependent correction in the offset (a_0) term is applied in C7 for all TEB, except for bands 21 and 31. Figure 14 shows an example of Aqua band 20, which demonstrates a significant reduction in the BT difference after implementation of the a_0 correction in C7. Results of the other bands show similar patterns.

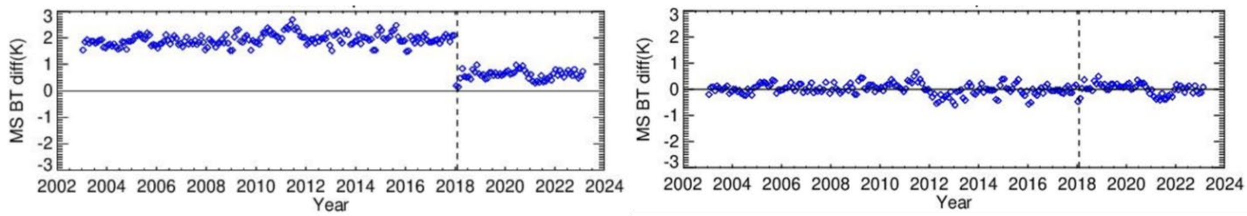

Fig. 14: (Left) Trend of mirror side BT differences over qDCC for Aqua band 20 from C6.1. (Right) Trend of mirror side BT differences over qDCC for Aqua band 20 from C7. Each symbol represents the monthly-averaged mirror-side differences. The vertical dashed line indicates the time of occurrence for the formatter reset (January 2018).

Even after correcting for the crosstalk impact on Aqua PV LWIR bands 27 to 30, calculated radiance measurements show a noticeable long-term drift for these bands, particularly after 2012. The assessment uses inputs from MODIS data trends over various targets (ocean, desert, Dome-C, and qDCC), along with cross-sensor comparison with the Infrared Atmospheric Sounding Interferometer (IASI) hyperspectral measurements onboard the EUMETSAT Polar System MetOp (Meteorological Operational) series. Results show that the drifts are BT-dependent with temporal changes up to 0.75 K over the entire mission. In C7, BB cool-down measurements are used to derive the non-linear (a_2) coefficients, instead of the on-orbit adjustment of the prelaunch coefficients as was implemented in C6.1. This approach enables a more accurate estimation of the on-orbit changes. In addition, to improve the long-term stability in the bands 27-30, the non-linear (a_2) coefficients from 2012 to present time are held fixed at a constant value – the value derived from the cool-down measurements as of 2012. With the implementation of the crosstalk correction and the special consideration for the a_2 coefficients, the observed drifts for these bands were largely reduced to well within 0.5 K over the entire mission.

5 Lessons and Future Considerations

Several lessons have been learned over the 20 years of on-orbit operation of Aqua MODIS. The on-orbit calibration of Aqua MODIS has significantly benefitted from the experiences gained from the on-orbit calibration and performance of the MODIS instrument onboard the Terra spacecraft. In particular, the on-orbit calibration algorithms for the RSB RVS and the electronic crosstalk characterization in the TEB have been inherited from Terra MODIS. In this section, we summarize some of the remaining challenges facing both the RSB and TEB.

The changes in the Aqua orbit will result in changes to data collection from all calibration sources used in Aqua RSB calibration, including the SD, Moon, and desert sites. Changes to the desert site observations, critical for the RVS characterization of VIS/NIR bands, began in February 2022 when the Aqua ground track moved out of its historic repeated pattern. Several options are being explored to ensure continuity of calibration through the orbit drift such as the use of DCC and/or the Dome-C site located near the south pole, which will have more observation opportunities. As Aqua MODIS continues to age, it is possible that the existing EV-based calibration may need to be extended to additional bands, for example band 10. Use of different desert sites, or inter-band calibration over ocean scenes, are options. The Moon has been viewed within a constrained phase angle range via regularly scheduled spacecraft roll maneuvers with the changes in the view geometry accounted by the USGS ROLO model. Starting 2022, the orbital maintenance maneuvers for Aqua are no longer performed therefore limiting the number of observations within the previous phase angle ranges. Work is underway to develop a correction based on unscheduled Moon measurements that cover a range of phase angles to avoid any observed biases in the gains derived from the lunar measurements [33]. We will also continue to monitor band/detector performance for any unexpected increases in the polarization sensitivity or crosstalk, and the continued degradation of the SD. Fortunately, for many of these concerns, successful mitigation algorithms have already been developed and applied for Terra MODIS and could be extended to Aqua, if needed. Some additional concerns that have been previously identified for select Aqua RSB include changes in relative spectral response (bands 8 and 9) and radiance-dependent gain changes (bands 1 and 2) [34]. Mitigation strategies for these impacts have been developed and could be considered for future implementation. Early mission yaw maneuvers were performed to characterize the SD screen vignetting function and the SD BRF, including at the SDSM view angle. There is a consideration to perform another set of yaw maneuvers to extend (or shift) the geometric range of SD screen vignetting function and the SD BRF characterization and to evaluate mission-long changes in these parameters.

Electronic crosstalk contaminations have had an impact on the Aqua TEB calibration and Earth-view measurements. The crosstalk correction algorithm, previously developed for Terra MODIS, has been applied in C7 to select MWIR detectors and the PV LWIR bands and significantly improves the quality of the L1B product. The electronic crosstalk characterization relies on scheduled lunar measurements, and with the possibility of diminished opportunities of lunar observations, alternative means of deriving electronic crosstalk will be explored. As discussed earlier, the Aqua MODIS CFPA cooler margin significantly improved after the April 2022 safe hold that involved a mid-mission outgassing. MCST will continue to monitor the cooler margin and its trend, as well as other parameters sensitive to the CFPA temperatures. A spacecraft pitch maneuver was performed in August 2021 where the TEB viewed the deep-space that enabled the on-orbit characterization of their RVS. Results show that the deep-space calibration derived RVS agrees with the prelaunch result to within 0.3% over the entire EV scan angle range for all TEB except bands 29 and 30 which show some divergence of 0.5% at the AOI of 50°. Further assessments from EV measurements did not show these divergences and indicated that the Aqua TEB RVS is stable over the mission and no additional on-orbit adjustment is required.

6 Summary

Aqua MODIS has completed over 20 years of successful on-orbit operation providing the science community with a high-quality data record of Earth observations supporting multiple applications. All the OBC, including the SD, SDSM, BB, and SRCA, continue to be routinely operated and are used to provide the baseline calibration and characterization of Aqua MODIS. The dedicated calibration efforts undertaken by the MCST utilize the measurements from the OBC, lunar observations, and Earth observations to monitor and improve the MODIS calibration. Some of the calibration algorithms implemented over the years include upgrades to the RSB RVS characterization and improvements in the electronic crosstalk characterization in the TEB. As the Aqua spacecraft continues to drift away from its nominal orbit, additional adjustments to the SD and lunar calibrations will be necessary, the strategies for which have already been formulated and implemented.

Code, Data, and Materials Availability

All data presented in this article were derived from the Aqua MODIS Level 1A and L1B files, which were publicly available through the NASA MODIS Adaptive Processing System (MODAPS), Goddard Space Flight Center, USA, DOI 10.5067/MODIS/MYD01.061, 10.5067/MODIS/MYD021KM.061, 10.5067/MODIS/MYD002OBC.061

7 Acknowledgements

The authors would like to thank other members of the MODIS Characterization Support Team, Raytheon MODIS Support Team, and MODIS Science Team for their technical assistance and support. The authors would also like to thank Dr. Truman Wilson for a technical review of this manuscript.

References

1. V. Salomonson, W. Barnes, P. W. Maymon, H. Montgomery, and H. Ostrow, "MODIS: Advanced Facility Instrument for Studies of the Earth as a System", *IEEE Trans. Geosci. Remote Sens*., **27**,2, pp. 145-153, (1989).
2. W.L. Barnes and V.V. Salomonson, "MODIS: A global image spectroradiometer for the Earth Observing System," *Critical Reviews of Optical Science and Technology*, **CR47**, 285-307 (1993).
3. V.V. Salomonson, W.L. Barnes, X. Xiong, S. Kempler, and E. Masuoka, "An Overview of the Earth Observing System MODIS Instrument and Associated Data Systems Performance", *Proceedings of IGARSS*, **2**, 1174 – 1176 (2002).
4. X. Xiong , M. D. King, V. Salomonson, W. Barnes, B. N. Wenny, A. Angal, A. Wu, S. Madhavan, and D. Link, "Moderate Resolution Imaging Spectroradiometer on Terra and Aqua Missions", *John Wiley & Sons, Ltd*, **9781118945179**, 53-89, (2015).
5. X. Xiong, K. Chiang, N. Chen, S. Xiong, W.L. Barnes, B. Guenther, " Results and lessons from MODIS thermal emissive bands calibration: pre-launch to on-orbit", *Proc. SPIE*, *Earth Observing Systems XI*, **6296**, 62960A, (2006).
6. X. Xiong, N. Che, C. Pan, X. Xie, J. Sun, W.L. Barnes, B. Guenther, " Results and lessons from MODIS reflective solar bands calibration: pre-launch to on-orbit", *Proc. SPIE*, *Earth Observing Systems XI*, **6296**, 629607, (2006).

7. A. Angal, X. Xiong, T. Chang, K. Twedt, X. Geng, A. Wu, E. Aldoretta, "Terra and Aqua Moderate-resolution Imaging Spectroradiometer Collection 7 Level 1B Algorithm," Journal of Applied Remote Sensing, **16**, 3, (2022).
8. X. Xiong, A. Angal, K. A. Twedt, H. Chen, D. Link, X. Geng, E. Aldoretta, Q. Mu, "MODIS Reflective Solar Bands On-Orbit Calibration and Performance", *IEEE Transactions on Geoscience and Remote Sensing,* **57**, 9, 6355-6371, (2019).
9. X. Xiong, A. Wu, T. Chang, T. Wilson, Y. Li, N. Chen, A. Shrestha, C. Diaz, "On-orbit calibration and performance assessments of Terra and Aqua MODIS thermal emissive bands", Journal of Applied Remote Sensing, **15**, 1, (2021).
10. X. Xiong, W. Barnes, B. Guenther, and R. E. Murphy, "Lessons Learned From MODIS", *Adv. Space Res.*, **32**, 11, 2107-2112 (2003).
11. J. Sun, X. Xiong, W. Barnes, and B. Guenther, "MODIS Reflective Solar Bands On-Orbit Lunar Calibration", *IEEE Trans. Geosci. Remote Sens*., **45**,7, 2383-2393, (2007).
12. X. Xiong, N. Che, and W. Barnes, "Terra MODIS On-Orbit Spatial Characterization and Performance", *IEEE Trans. Geosci. Remote Sens*., **43**, 2, 355-365, (2005).
13. X. Xiong, N. Che, and W. Barnes, "Terra MODIS On-Orbit Spectral Characterization and Performance", *IEEE Trans. Geosci. Remote Sens*., **44** ,8, 2198-2206, (2006).
14. Z. Wang, S. Madhavan, X. Xiong, A. Wu, B. Wenny, " Monitoring and assessment of the temperature fluctuation of Aqua MODIS cold focal plane assembly", *Proc. SPIE*, *Earth Observing Systems XVII*, **8510**, 85100K, (2012).
15. X. Xiong, A. Angal, J. Sun, T. Choi, E. Johnson, "On-orbit performance of MODIS solar diffuser stability monitor," Journal of Applied Remote Sensing, **8**, 083514, (2014).
16. H. Chen, X. Xiong, A. Angal, K. Twedt, "On-orbit Characterization of the MODIS SDSM Screen for Solar Diffuser Degradation Estimation," *IEEE Transactions on Geoscience and Remote Sensing*, **55**,11, 6456-6467, (2017).

17. K. Twedt, A. Angal, X. Xiong, X. Geng, H. Chen, " MODIS solar diffuser degradation at short-wave infrared band wavelengths", *Proc. SPIE*, *Earth Observing Systems XXII*, **10402**, 104022K, (2017).

18. J. Sun, X. Xiong, A. Angal, H. Chen, A. Wu, and X. Geng, “Time-Dependent Response Versus Scan Angle for MODIS Reflective Solar Bands,” *IEEE Transactions on Geoscience and Remote Sensing*, **52,6,** 3159–3174, (2014).

19. A. Angal X. Xiong, A. Wu, X. Geng, H. Chen, “Improvements in the On-Orbit Response Versus Scan Angle Characterization of the Aqua MODIS Reflective Solar Bands”, *IEEE Transaction on Geoscience and Remote Sensing,* **56**, 3, 1728-1738, (2018).

20. E. Kwiatkowska, B. Franz, G. Meister, C. McClain, and X. Xiong, "Cross calibration of ocean-color bands from Moderate Resolution Imaging Spectroradiometer on Terra platform," *Appl. Opt.* **47**, 6796-6810, (2008).

21. Meister, G., R. E. Eplee, B. A. Franz, "Corrections to MODIS Terra calibration and polarization trending derived from ocean color products," Proc. SPIE, Earth Observing Systems XIX, 9218, 92180V (2 October 2014)

22. A. Angal, X. Xiong, J. Sun, and X. Geng, "On-orbit noise characterization of MODIS reflective solar bands", *J. Appl. Remote Sens*., **9**, 1, (2015).

23. X. Xiong, A. Angal, W. L. Barnes, H. Chen, V. Chiang, X. Geng, Y. Li, K. Twedt, Z. Wang, T. Wilson, et al., "Updates of Moderate Resolution Imaging Spectroradiometer on-orbit calibration uncertainty assessments", Journal of Applied Remote Sensing, 12, 3,034001, (2018).

24. X. Xiong, B. N. Wenny, A. Wu, W. L. Barnes, and V. V. Salomonson, “Aqua MODIS Thermal Emissive Band On-Orbit Calibration, Characterization, and Performance”, *IEEE Transactions on Geoscience and Remote Sensing*, **47**, 3, 803-814, (2009).

25. G. R. Keller, T. Wilson, X. Geng, A. Wu, Z. Wang, and X. Xiong, “Aqua MODIS Electronic Crosstalk Survey: Mid-Wave Infrared Bands”, *IEEE Transactions on Geoscience and Remote Sensing*, **57**, 3, 1684-1697, (2019).

26. S. Madhavan, X. Xiong, A. Wu, B. N. Wenny, K. Chiang, N. Chen, Z. Wang, and Y. Li, "Noise Characterization and Performance of MODIS Thermal Emissive Bands", *IEEE Transactions on Geoscience and Remote Sensing*, **54**, 6, 3221-3234, (2016).
27. D. Link, X. Xiong, and Z. Wang, "Assessment of MODIS on-orbit spatial performance", *Proc. SPIE Sensors, Systems, and Next-Generation Satellites XIX,* **9639**, 963910, (2015).
28. E. Aldoretta, D. Link, K. Twedt, X. Xiong, "Twenty years of Terra MODIS spectral performance using the spectro-radiometric calibration assembly", *Proc. SPIE, Earth Observing Systems XXV*, **11501**, 115010D, (2020).
29. G. Toller, X. Xiong, J. Sun, B. N. Wenny, X. Geng, J. Kuyper, A. Angal, H. Chen, S. Madhavan, and A. Wu, "Terra and Aqua Moderate-resolution Imaging Spectroradiometer Collection 6 Level 1B Algorithm," *Journal of Applied Remote Sensing*, **7**, 1, (2013).
30. T. Wilson, A. Wu, A. Shrestha, X. Geng, Z. Wang, C. Moeller, R. Frey, and X. Xiong, "Development and implementation of an electronic crosstalk correction for bands 27-30 in Terra MODIS collection 6," *Remote Sens.* **9**, 6, 569, (2017).
31. K. Twedt, E. Aldoretta, A. Angal, H. Chen, X. Geng, Y. Li, Q. Mu, K. Vermeesch, X. Xiong, "MODIS reflective solar bands calibration improvements for Collection 7", *Proc. SPIE Sensors, Systems, and Next-Generation Satellites XXV*, **11858**, 118580S, (2021).
32. T. Chang, A. Shrestha, C. Perez Diaz, N. Chen, A. Wu, T. Wilson, Y. Li, X. Xiong, "MODIS thermal emissive bands calibration improvements for Collection 7", *Proc. SPIE Sensors, Systems, and Next-Generation Satellites XXV*, **11858**, 118580R, (2021).
33. X. Xiong, J. Sun, A. Angal, T. Wilson, "Calibration Inter-Comparison of MODIS and VIIRS Reflective Solar Bands Using Lunar Observations", *Remote Sensing*, **14**, 21, 4754, (2022)
34. S. Lee and G.Meister, "MODIS Aqua Optical Throughput Degradation Impact on Relative Spectral Response and Calibration of Ocean Color Products", *IEEE Transactions on Geoscience and Remote Sensing*, **55**, 9, 5214-5219, (2017).

Dr. Xiaoxiong (Jack) Xiong is an optical physicist in the Sciences and Exploration Directorate at NASA's Goddard Space Flight Center, currently supporting Terra, Aqua, S-NPP, and JPSS missions/projects on sensor calibration and characterization. He has served as the Technical Lead for the MODIS Characterization Support Team (MCST) since 2003, Technical Lead for the VIIRS Characterization Support Team (VCST) since 2004, and MODIS Project Scientist for instrument operation and calibration since 2005. He is also a member of the CLARREO Science Definition Team and CLARREO Pathfinder Team. He received a B.S. degree in optical engineering from Beijing Institute of Technology and a Ph.D degree in physics from University of Maryland. Before joining NASA, he had also worked in the fields of optical instrumentation, nonlinear optics, laser and atomic spectroscopy, and resonance ionization mass spectrometry at US private companies, at the University of Maryland, College Park and the National Institute of Standards and Technology (NIST). Dr. Xiong has been serving as the co-chair for the SPIE conference on Earth Observing System since 2006 and for the SPIE conference on Earth Observing Missions and Sensors: Development, Implementation, and Characterization since 2010.

35. http://science.gsfc.nasa.gov/sed/bio/xiaoxiong.xiong-1

36.

Biographies and photographs for the other authors are not available.

Caption List

Fig. 1 (left) Aqua MODIS instrument (black) and VIS FPA (blue) temperature trends. (right) Aqua MODIS short and midwave infrared (SMIR; red) and longwave infrared (LWIR; blue) FPA temperature trends. Red vertical dotted lines represent safe hold occurrences.

Fig. 2 Degradation in the reflectance of the solar diffuser over the mission as measured by the SDSM. (Left) The measured SD degradation at SDSM detectors 1, 3, and 7 as a function of time. (Right) The SD degradation as a function of wavelength for three select years during the mission. Red vertical dotted lines represent safe hold occurrences.

Fig. 3 On-orbit gain changes for VIS bands 8, 3, and 4 from (left) SD measurements and (right) lunar observations. Red vertical dotted lines represent safe hold occurrences.

Fig. 4 On-orbit gain changes from SD measurements for (left) NIR bands 1, 2, 16, and 19 and (right) SWIR bands 5, 7, and 26. Red vertical dotted lines represent safe hold occurrences.

Fig. 5 RVS for (left) band 8, (center) band 3, and (right) band 1 at three different times in the mission. By definition, the RVS is normalized to the SD frame (978).

Fig. 6 Aqua MODIS RSB uncertainty at nadir (typical radiance) for select years. The horizontal red line indicates the specified 2% uncertainty requirement.

Fig. 7 (Left) Trend of Aqua BB temperature over the mission. Data are collected at weekly intervals. (Right) BB temperature collected using 200 consecutive granules on July 3, 2022. Red vertical dotted lines represent safe hold occurrences.

Fig. 8 (Left) Trends of normalized 1/ b_1 (gain) over the mission for Aqua bands 20, 27, 31 and 35. Data are collected at weekly intervals. (Right) Normalized b_1 for the same four bands collected using 200 consecutive granules on July 3, 2022. Red vertical dotted lines represent safe hold occurrences.

Fig. 9 Aqua MODIS TEB uncertainty at nadir (typical radiance) for the years 2002, 2012, and 2022. The horizontal red lines indicate the specified uncertainty requirement for each band.

Fig. 10 The yearly-averaged BBR along-scan (left) and along-track (right) for all Aqua MODIS bands for select years.

Fig. 11 The yearly-averaged CW (left) and BW (right) changes in the Aqua MODIS RSB for select years.

Fig. 12 : (Left) Libya 4 reflectance trends for Aqua band 8 mirror side 1 frame 731 (near nadir) for Collection 6.1 compared to Collection 7. (Right) Comparison of C6.1 to C7 reflectance mirror side ratio.

Fig. 13: (Left) Comparison of histograms for Aqua band 24 detector 1 before and after the electronic crosstalk correction using granule 2023034.0020. (Right) Comparison of histograms for all detectors of Aqua band 27 using granule 2023062.1200.

Fig. 14: (Left) Trend of mirror side BT differences over qDCC for Aqua band 20 from C6.1. (Right) Trend of mirror side BT differences over qDCC for Aqua band 20 from C7. Each symbol represents the monthly-averaged mirror-side differences. The vertical dashed line indicates the time of occurrence for the formatter reset (January 2018).

Table 1 Key design parameters for the MODIS spectral bands

Table 2 Major Events for Aqua MODIS

Table 3 Aqua MODIS on-orbit calibration activities (as of March 31, 2023)

Table 4 RSB SNR Performance at typical radiance. Yearly-averaged results are shown relative to their band specification.

Table 5. Aqua MODIS TEB noise performance (at typical temperature) for select years